Available online at www.sciencedirect.com

SciVerse ScienceDirect

Geochimica et Cosmochimica Acta 75 (2011) 6912–6926

Geochimica et Cosmochimica Acta

www.elsevier.com/locate/gca

Stable isotopes and the noncarbonaceous derivation of ureilites, in common with nearly all differentiated planetary materials

Paul H. Warren

Institute of Geophysics and Planetary Physics, University of California, Los Angeles, CA 90095-1567, United States

Received 28 April 2011; accepted in revised form 6 September 2011

Abstract

The abundant, diverse ureilite meteorites are peridotitic asteroidal mantle restites that have remarkably high bulk carbon contents (average 3 wt%) and have long been linked to the so-called carbonaceous chondrites (although this term is potentially misleading, because the high petrologic type "carbonaceous" chondrites are, if anything, C-poor compared to ordinary chondrites). Ureilite oxygen isotopic compositions, i.e., diversely negative (CCAM-like) $\Delta^{17}O$, viewed in isolation, have long been viewed as confirming the carbonaceous-chondritic derivation hypothesis. However, a very different picture emerges through analysis of a compilation of recently published high-precision isotopic data for chromium, titanium and nickel for ureilites and various other planetary materials. Ureilites have lower $\varepsilon^{62}Ni$ and far lower $\varepsilon^{50}Ti$ and $\varepsilon^{54}Cr$ than any known variety of carbonaceous chondrite. On a plot of $\varepsilon^{50}Ti$ vs. $\varepsilon^{54}Cr$, and similarly $\Delta^{17}O$ vs. $\varepsilon^{54}Cr$, ureilite compositions cluster far from and in a direction approximately orthogonal to a trend internal to the carbonaceous chondrites, and the carbonaceous chondrites are separated by a wide margin from all other planetary materials. I conclude that notwithstanding the impressive resemblance to carbonaceous chondrites in terms of diversely negative $\Delta^{17}O$, the ureilite precursors accreted from preponderantly noncarbonaceous (sensu stricto) materials. Despite total depletion of basaltic matter, the ureilites retain moderate pyroxene/olivine ratios; which is an expected outcome from simple partial melting of moderate-SiO_2/(FeO + MgO) noncarbonaceous chondritic material, but would imply an additional process of major reduction of FeO if the precursor material were carbonaceous-chondritic. The striking bimodality of planetary materials on the $\varepsilon^{50}Ti$ vs. $\varepsilon^{54}Cr$ and $\Delta^{17}O$ vs. $\varepsilon^{54}Cr$ diagrams may be an extreme manifestation of the effects of episodic accretion of early solids in the protoplanetary nebula. However, an alternative, admittedly speculative, explanation is that the bimodality corresponds to a division between materials that originally accreted in the outer solar system (carbonaceous) and materials that accreted in the inner solar system (noncarbonaceous, including the ureilites).

1. INTRODUCTION

An exemplary case of exploiting stable isotopes to constrain the diverse derivations of planetary materials was Clayton and Mayeda's (1988) pioneering study of the ureilite meteorites. Ureilites are extremely depleted asteroidal peridotites (when reviewed by Goodrich et al. (2004), the number of ureilites had reached ~100; it has roughly doubled since; among achondrites, only HEDs are more common). Early petrologic models envisaged the ureilites as extensively metamorphosed and recrystallized chondrites (Ringwood, 1960; Wlotzka, 1972). Then, for some years, models for ureilite genesis as cumulates from intrusive magmas (e.g., Berkley et al., 1980; Goodrich et al., 1987) competed with the view (e.g., Boynton et al., 1976; Takeda, 1987) that ureilites formed as anatectic (partial melting) mantle restites. The restite model, by virtue of its consistency with limited stirring of the materials within the parent asteroid, was essentially confirmed by Clayton and Mayeda's (1988) discovery that great oxygen-isotopic diversity is preserved among the ureilites. There is now a general consensus that at least most of the ureilites formed as restites (e.g., Warren and Kallemeyn, 1992; Scott et al.,

E-mail address: pwarren@ucla.edu

0016-7037/$ - see front matter © 2011 Elsevier Ltd. All rights reserved.
doi:10.1016/j.gca.2011.09.011

1993; Singletary and Grove, 2003; Goodrich et al., 2004; Kita et al., 2004; Warren and Huber, 2006).

Ureilites are still the only differentiated meteorite type known to encompass a large range of oxygen-isotopic composition. Ureilites also show considerable diversity in terms of their modal proportions of olivine and pyroxenes (pigeonite, orthopyroxene and augite), and in the compositions of these silicates (e.g., olivine ranges from Fo_{75} to Fo_{96}). Yet they are remarkably consistent in several important respects. Almost every ureilite contains an important proportion (average 3 wt%: Warren and Huber, 2006) of interstitial carbon (including crystalline graphite, diamond and lonsdaleite: Mittlefehldt et al., 1998). The rims of ureilite olivines show distinctive indications of late FeO reduction: tiny inclusions of Fe-metal scattered amidst olivine that is reversely zoned toward pure Mg–olivine. In contrast, the mafic-silicate cores in any individual monomict ureilite are remarkably uniform in composition. Nearly all ureilites exhibit a remarkably step-wise cooling history: slow at first, but very rapid later (Miyamoto et al., 1985; Takeda et al., 1989; Herrin et al., 2010).

Many authors have assumed that ureilite traits such as high bulk carbon contents and diverse, ^{16}O-rich oxygen isotopic compositions imply a link with the carbonaceous chondrites (e.g., Mueller, 1969; Vdovykin, 1970; Higuchi et al., 1976; Wasson et al., 1976; Berkley et al., 1980; Takeda, 1987; Rubin, 1988; Ikeda and Prinz, 1993; Goodrich et al., 2002, 2007; Kita et al., 2004). However, as this paper will review, a variety of recent high precision stable-isotopic measurements, when assessed in aggregate, call the carbonaceous chondrite derivation hypothesis into question. The ureilite parent body probably formed as a mixture of various precursor materials (as became clear with the discovery of the ureilites' great O-isotopic diversity: Clayton and Mayeda, 1988), and none of those precursors, let alone their aggregate, was likely a close match with any known chondrite. Nonetheless, it is worthwhile to look for evidence as to which general type of material dominated the mix.

A few words about nomenclature: It is self-evident that as relatively carbon-rich meteorites ureilites may be said to be carbonaceous, in a layman's sense of that word. However, it has long been customary in meteorite classification to describe as "carbonaceous" a distinctive set of chondrites that are similar in various ways but not necessarily carbon-rich. The term is "somewhat of a misnomer" (Krot et al., 2004). Other, less elastic "carbonaceous" characteristics have seldom been enumerated (the words of Justice Potter Stewart, "I know it when I see it," come to mind), but according to Krot et al. (2004; cf. Weisberg et al., 2006) they include: ^{16}O-rich oxygen isotopic composition (except in the case of CI); CI-or-higher mean ratio of refractory lithophile elements to the major lithophile element Si; relatively high abundance of refractory inclusions (except in CI); and high matrix/chondrule abundance ratio. Henceforward in this paper, the word carbonaceous will be used in that restricted, meteoritics-customary sense.

2. DATA SOURCES

Oxygen isotopic data are taken almost exclusively from an extensive compilation of data from the Clayton–Mayeda team (e.g., Clayton and Mayeda, 1988, 1996; Clayton et al., 1976, 1991). For ureilites, Clayton's data are augmented by a precise but not well documented data set from Franchi et al. (1998; data are shown with no indication of which ureilites they represent), by seven analyses of NWA ureilites listed in the *Meteoritical Bulletin*, and by one analysis (Sahara 99201) by Smith et al. (2001). Ureilite olivine-core Fo and modal data are mainly from the compilation of Mittlefehldt et al. (1998) along with newer data from the *Meteoritical Bulletin*.

Chromium isotopic data are taken from Bogdanovski and Lugmair (2004), Yamashita et al. (2005), Shukolyukov and Lugmair (2006a,b), Ueda et al. (2006), Trinquier et al. (2007, 2008), Yin et al. (2009), de Leuw et al. (2010), Qin et al. (2010a,b), Shukolyukov et al. (2011), and especially, as the main source of bulk-ureilite measurements, (Yamakawa et al., 2010). The ordinary chondrite data of de Leuw et al. (2010) seem aberrant and were excluded. The effect of including them would be to cause the H, L and LL ε^{54}Cr means to be lower by relatively insignificant extents, from −0.34, −0.40 and −0.40, to −0.55, −0.67 and −0.81, respectively.

Nickel isotopic data are taken from Regelous et al. (2008), Dauphas et al. (2008) and Quitté et al. (2010). The data of Bizzarro et al. (2007) are problematical (Dauphas et al., 2008) and were not utilized in this work (for the record, the great ε^{62}Ni diversity they found would, if real, only tend to strengthen this paper's main conclusions). With that qualification, meteorites that have been analyzed for ε^{62}Ni include four ureilites, all by Quitté et al. (2010). However, ureilites are not Ni-rich materials, and the individual ureilite ε^{62}Ni uncertainties (average: 0.56) are comparable to the total ε^{62}Ni range among all bulk meteorites.

Titanium isotopic data are from just two sources: Leya et al. (2008) and Trinquier et al. (2009). Many of the data of Trinquier et al. (2009) were obtained as replicates at two separate labs, with good agreement between the two sets of results. The suite of meteorites analyzed by Leya et al. included three ureilites, and Trinquier et al. analyzed (twice) NWA 2376.

For chondrite and ureilite bulk-oxide compositions, I rely primarily (exceptions will be noted) on the excellent data compilation of Jarosewich (1990; with minor updates by Jarosewich, 2006). Most other bulk-meteorite analyses are incomplete inasmuch as they do not distinguish between the various oxidation states of iron. Additional wet-chemical analyses are scattered in the literature, but Jarosewich's data are known to be of consistently high quality, they are sufficient for most purposes, and this approach has the advantage of minimizing interlaboratory bias.

The distribution of the ε^{50}Ti, ε^{54}Cr and ε^{62}Ni data sources by meteorite type is shown in Table EA-1 of this paper's Electronic Annex. For plotting purposes, I have first averaged data for individual meteorites, and then averaged those results to arrive at averages for each meteorite variety (except for ureilites, plotted individually).

3. COSMOCHEMICAL DESCENT OF THE UREILITES

3.1. Oxygen isotopes, considered in isolation

Fig. EA-1 in the Electronic Annex to this paper shows a compilation of data on the classic diagram for application of stable isotopes to the issue of meteorite pedigree (Clayton et al., 1973), a plot of $\delta^{18}O$ vs. $\delta^{17}O$. Ureilites, and as yet no other known type of achondrite, display a trend with approximately +1 slope on Fig. EA-1 and a wide variation in $\Delta^{17}O$ ($\equiv \delta^{17}O - 0.52\ \delta^{18}O$; where 0.52 is the slope of kinetic mass fractionation, including the Terrestrial Fractionation Line, TFL). This trend is approximately a higher-$\Delta^{17}O$ extension of the trend defined by the CV and CO analyses, the CCAM (carbonaceous chondrite anhydrous minerals) line. This aspect of resemblance to the carbonaceous chondrites is often cited (e.g., Rubin, 1988; Goodrich, 1992) as suggestive of a genetic link between ureilites and carbonaceous chondrites. However, the anhydrous carbonaceous groups (CO, CK and CV) are not the only chondrites that exhibit a roughly +1 slope on the three-O-isotope diagram (Fig. EA-1). As shown by Clayton et al. (1991), the ordinary chondrites (OC), when viewed as a related set, also form a trend with slope ~ +1.07. Adherence to this relationship is closest among the more equilibrated petrologic types of OC, and Clayton et al. called this trend the "Equilibrated Chondrite Line" or ECL. A more up-to-date compilation for observed falls (compiled by J.T. Wasson; still exclusively Clayton-lab data) modifies the ECL slope to 0.90. Among the OC, the group with the most oxidized, FeO-rich silicates, LL, plots at the high $\Delta^{17}O$ end of the ECL; the group with the most FeO-poor silicates, H, forms the low $\Delta^{17}O$ end. As noted by Goodrich and Delaney (2000), this situation is analogous with the ureilites: those with the most FeO-rich silicates plot toward the high $\Delta^{17}O$ end of a diffuse yet significant anticorrelation between $\Delta^{17}O$ and olivine-core Fo (Fig. 1). Among the carbonaceous chondrites, the groups with the highest carbon contents (data of Jarosewich, 1990) do not belong to the subset that exhibit +1 slopes on the three-O-isotope diagram (Fig. EA-1). The CI (average 2.8 wt% C) and CM (1.7 wt%) groups exhibit slopes that are poorly defined but closer to +0.52 (the TFL) than to +1. The CR (2.0 wt%) group exhibits an intermediate slope of ~+0.75 (Choi et al., 2009). The groups that exhibit +1 slopes, CO–CK–CV, only contain from 0.03 to 0.54 wt% carbon. (The issue of the relationship between oxygen isotopes and initial bulk carbon content will be revisited in Section 4.)

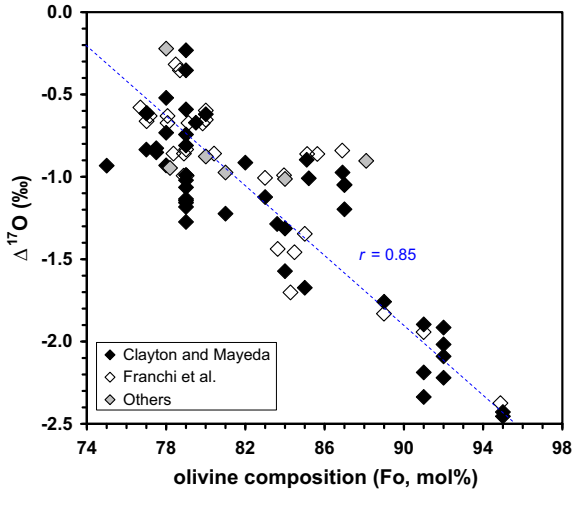

Fig. 1. Ureilite olivine-core Fo vs. $\Delta^{17}O$. Despite a distinctive "Hughes cluster" (Downes et al., 2008) near Fo_{87} and $\Delta^{17}O \approx -1.0$, the data show a strong overall anticorrelation. Regarding data sources for this and other figures involving $\Delta^{17}O$, see text.

The fact that among ureilites $\Delta^{17}O$ is consistently negative, and ranges from −0.2‰ to −2.45‰, is arguably more impressive evidence for the hypothesis of carbonaceous-chondritic derivation. However, the ureilite compositional distribution is skewed toward the ferroan (low-Fo) end (Goodrich et al., 2004; Downes et al., 2008), so that the average olivine-core composition of ~Fo81.5 corresponds, via Fig. 1, to a comparatively moderate $\Delta^{17}O$ of −1.0‰. The noncarbonaceous chondrites, which only comprise three main classes (OC, EC and R chondrites), have class-mean $\Delta^{17}O$ ranging from 0‰ to ~2.7‰. The Kakangari grouplet, whose place in meteorite classification is unclear although the grouplet is generally regarded as noncarbonaceous (Weisberg et al., 2006), arguably extends this range to −1.75‰ (Clayton et al., 1976; Weisberg et al., 1996). Even ignoring the Kakangari grouplet, postulating that a 4th class, the ureilite precursor materials, once extended the noncarbonaceous range by factor of ~1.4 is not, ipso facto, implausible.

The origin of the planetary-meteoritical $\Delta^{17}O$ diversity remains controversial. For most of the isotopic systems about to be discussed, the variations are generally assumed to reflect incomplete (and/or impermanent: Trinquier et al., 2009) mixing of stellar-nucleosynthetic ejecta. However, for oxygen, models range from episodic in-mixing of different reservoirs of stellar-nucleosynthetic origin (with perhaps a temporal trend toward higher $\Delta^{17}O$: Wasson, 2000), to "self shielded" ultraviolet photodissociation of CO, either in the parent molecular cloud (Yurimoto and Kuramoto, 2004) or within the solar nebula (e.g., Lyons and Young, 2005; Clayton, 2008).

3.2. Chromium and nickel isotopes

Fig. 2 shows $\varepsilon^{62}Ni$ plotted vs. $\varepsilon^{54}Cr$ (cf. analogous diagrams, based on smaller data sets, in Regelous et al. (2008) and Bizzarro et al. (2007); however, as mentioned previously, the $\varepsilon^{62}Ni$ data of Bizzarro et al. are not used in this work). The variations observed here are too great to be the result of mass fractionation. There is no doubt (e.g., Bizzarro et al., 2007; Dauphas et al., 2010; Qin et al., 2011) that these variations reflect an admixture of different nucleosynthetic components. In any case, these $\varepsilon^{54}Cr$ and $\varepsilon^{62}Ni$ isotopic variations, albeit discovered much later, are no less valid than the $\Delta^{17}O$ variations as indicators of planetary-material pedigree.

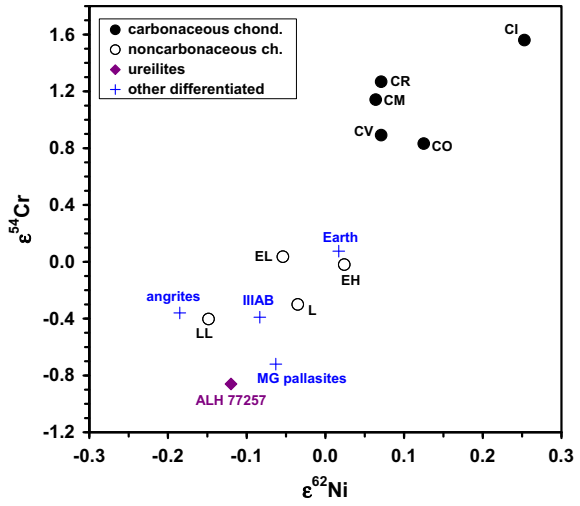

Fig. 2. Stable isotopic constraints: ε^{62}Ni vs. ε^{54}Cr. Data sources for ε^{62}Ni: Dauphas et al. (2008), Regelous et al. (2008) and Quitté et al. (2010); for more details, and for the numerous ε^{54}Cr data sources, see Table EA-1. Only one ureilite, ALH 77257, has been analyzed for both ε^{62}Ni and ε^{54}Cr. Three others (Quitté et al., 2010) have ε^{62}Ni of −0.60 to 0.07 (±0.48).

The overall pattern on a plot of ε^{62}Ni vs. ε^{54}Cr (Fig. 2) is a positive correlation. All five of the different analyzed carbonaceous chondrite groups are at the neutron-rich (in terms of ε^{62}Ni and ε^{54}Cr) end of the trend. The noncarbonaceous chondrite groups (EC and OC) are clustered toward the opposite end. Differentiated planetary materials, shown by crosses, tend to plot in the same low ε^{62}Ni, low ε^{54}Cr region. The one ureilite (ALH 77257) that has been analyzed for both ε^{62}Ni and ε^{54}Cr (Ueda et al., 2006; Quitté et al., 2010) plots at the extreme neutron-poor (low ε^{62}Ni, low ε^{54}Cr) end of the trend. That is, the opposite end from the carbonaceous chondrites. Regelous et al. (2008) found among four analyzed IVB irons a remarkably wide range in ε^{62}Ni, from −0.005 to 0.174 (±0.056). Unfortunately, no ε^{54}Cr (or ε^{50}Ti) data are available for IVB irons.

In terms of ε^{54}Cr alone (Fig. 3), among 13 analyzed ureilites the highest ε^{54}Cr result is −0.73 (MET78008; Ueda et al., 2006), and the average is -0.91 ± 0.20 (2σ). Among 22 analyzed carbonaceous chondrites the lowest ε^{54}Cr result is +0.33 (CK5 EET92002: Qin et al., 2010a), and the average is $+1.03 \pm (2\sigma)$ 0.61. When these data are run through the Kolmogorov–Smirnov test for data set comparison (Till, 1974), the results suggest that the probability for even the ureilite with the highest ε^{54}Cr (MET78008) to be of common derivation with carbonaceous-chondritic material is much less than 0.1%. Also, Qin et al. (2010b) measured ε^{54}Cr in a set of nine fragments of the Almahata Sitta polymict ureilite, and found a range of −0.85 to −0.67. Based on these data alone, Qin et al. (2010b) inferred that the ureilites "seem unlikely to be derived from any carbonaceous chondrite parent body".

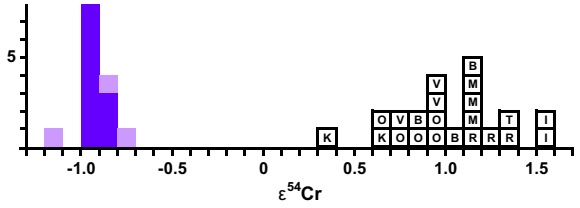

Fig. 3. Histogram of ureilite ε^{54}Cr data for carbonaceous chondrites (open symbols; letters indicate carbonaceous group; T indicates the CI-like but anomalous Tagish Lake) and ureilites (filled symbols). Regarding the numerous ε^{54}Cr data sources, see Table EA-1. Three early ureilite analyses from Ueda et al. (2006), which have especially high uncertainty, are denoted by lighter symbols.

3.3. Add titanium

Like oxygen, chromium and nickel, titanium shows great isotopic diversity among planetary materials. Leya et al. (2008) assumed the ε^{50}Ti diversity had a nucleosynthetic origin. However, Trinquier et al. (2009) found, by normalizing to the ^{49}Ti/^{47}Ti ratio, a correlation between ^{46}Ti and ^{50}Ti, which have different nucleosynthetic origins. These authors suggest that the protosolar molecular cloud may have once been well mixed, and invoke subsequent thermal processing to cause selective destruction of thermally unstable, isotopically anomalous presolar components. When Trinquier et al. (2009) analyzed acid-leach fractions from the Orgueil CI, they found a conspicuous lack of the ε^{46}Ti–ε^{50}Ti correlation that would be expected if mineralogically linked isotopic diversity had been engendered by kinetic-molecular mass fractionation. In any case, the ε^{50}Ti diversity clearly is not primarily due to mass fractionation, and can provide important insight regarding planetary-material genetic relationships.

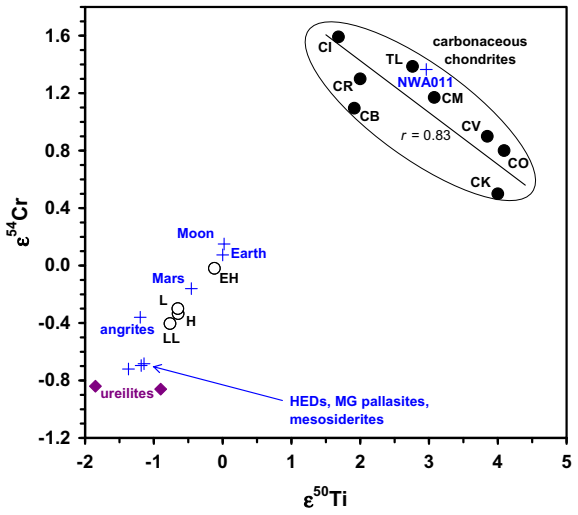

Fig. 4. Stable isotopic constraints: ε^{50}Ti vs. ε^{54}Cr. Symbols have same meanings as shown in Fig. 2. TL indicates the CI-like but anomalous Tagish Lake. Data sources for ε^{50}Ti: Leya et al. (2008) and Trinquier et al. (2009); for more details, and for the numerous ε^{54}Cr data sources, see Table EA-1. The two ureilites that have been analyzed for both ε^{50}Ti and ε^{54}Cr are ALH 77257 and NWA 2376.

A plot of ε^{50}Ti vs. ε^{54}Cr (Fig. 4; cf. Trinquier et al., 2009) roughly resembles Fig. 2: an overall positive correlation, with carbonaceous chondrites at the neutron-rich (high ε^{60}Ti, high ε^{54}Cr) end and ureilites at the opposite extreme. But Fig. 4 is even more inconsistent with a carbonaceous chondritic derivation for the ureilites. Among the carbonaceous chondrites, ε^{50}Ti vs. ε^{54}Cr manifests a significant, $r = 0.81$, anticorrelation; and the slope of this trend is approximately orthogonal to the overall trend that includes the ureilites and (other) "noncarbonaceous" materials. Thus, no realistic extension of the carbonaceous chondrite isotope-compositional distribution can be expected to incorporate the ureilites. Again, the other differentiated planetary materials plot in the same general region as the ureilites, but ureilites constitute the extreme "anti-carbonaceous" end of the differentiated range.

3.4. Oxygen, revisited

Additional insights are obtained by combining these isotopic systems with oxygen. Fig. 5 plots Δ^{17}O vs. ε^{54}Cr (cf. Fig. 2 of Trinquier et al., 2007; Fig. 3 of Qin et al., 2010b). Here, the distinction between the carbonaceous and noncarbonaceous chondrites is particularly clear because, among the carbonaceous chondrites, there is again a strong correlation, and the slope of this carbonaceous chondritic trend is approximately orthogonal to the direction toward the central portion of the range of noncarbonaceous chondrites. Except for the Eagle Station pallasites (actually only Eagle Station itself has thus far been analyzed: Shukolyukov and Lugmair, 2006b), the differentiated planetary materials again plot with the noncarbonaceous

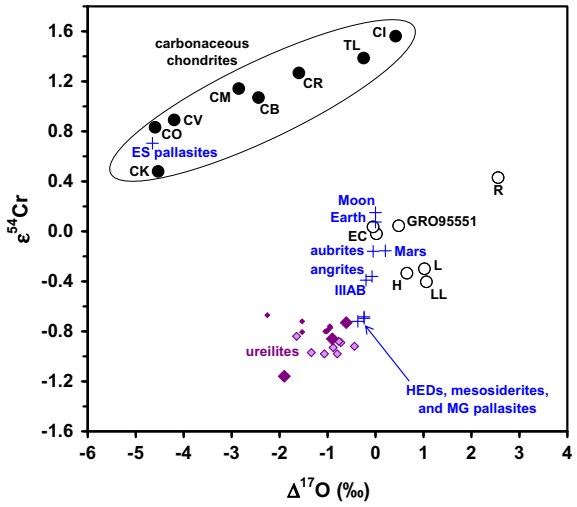

Fig. 5. Stable isotopic constraints: Δ^{17}O vs. ε^{54}Cr. Among the ureilite data, smaller diamonds represent diverse clasts from the Almahata Sitta polymict ureilite analyzed by Qin et al. (2010b); light-colored symbols represent instances where, in order to include some additional whole-rock ureilite ε^{54}Cr analyses, Δ^{17}O has been extrapolated from olivine-core Fo data based on the regression shown in Fig. 1. The only three ureilites that have been analyzed for both Δ^{17}O and ε^{54}Cr are ALH 77257, MET 78008, and Y-791538. (For interpretation of the references to color in this figure legend, the reader is referred to the web version of this article.)

chondrites. Together, the "noncarbonaceous" chondrites and differentiated materials (excluding Eagle Station) form a positive correlation that nearly parallels the trend of the carbonaceous chondrites. Admittedly, without the single R chondrite point, and/or without the ureilites, this trend would disappear. Still, by the simplest interpretation of Fig. 5 the ureilites represent the ^{16}O-rich end of a "noncarbonaceous" trend that may be analogous to the carbonaceous chondritic trend, including the similarity that in both cases the materials towards the low-ε^{54}Cr, ^{16}O-rich end of the trend are the ones that exhibit most clearly a slope of approximately +1 on Fig. EA-1.

GRO95551 is a metal-rich chondrite that superficially resembles the CB group (Mason, 1997). Weisberg et al. (2001) concluded on the basis of oxygen and nitrogen isotopes as well as mineral composition data that GRO95551 represents "a different nebular reservoir" from the CB group. The Cr data of Qin et al. (2010a) confirm this conclusion.

A plot of Δ^{17}O vs. ε^{62}Ni (Fig. EA-2) is qualitatively similar to Fig. 5. However, the carbonaceous-chondritic trend is relatively flat and the hiatus between the two fundamental material types is hardly noticeable. Even so, the few analyzed ureilites plot far from the carbonaceous-chondritic field. A plot of Δ^{17}O vs. ε^{50}Ti (Fig. EA-3) is also not particularly revealing, except in one respect. The NWA 011 basaltic achondrite (Yamaguchi et al., 2002; analyzed for ε^{50}Ti by Trinquier et al. (2009), as the NWA 2976 pair) shows clear evidence of a carbonaceous-chondritic pedigree.

3.5. The isotopic evidence as a whole

To summarize, viewed in isolation, the ureilites' low Δ^{17}O and roughly +1 slope on the three-O-isotope diagram (i.e., their nearness to the CCAM line; but the +1 slope is a trait shared with OC) might suggest a linkage with carbonaceous chondrites. Several far less ambiguous lines of evidence point toward the opposite inference of a pedigree closer to noncarbonaceous chondrites. Particularly telling are plots of Δ^{17}O vs. ε^{54}Cr (Fig. 5) and ε^{50}Ti vs. ε^{54}Cr (Fig. 4), where the ureilites plot not only far from, but also in an orthogonal direction from, the carbonaceous-chondritic trend. In these respects, ureilites are the extreme exemplars of a pattern of isotopic characteristics common to the majority of differentiated materials; the only known exceptions being the Eagle Station pallasites and the NWA 011 basaltic achondrite.

Carbon isotopes are unfortunately not very useful for constraining kinship among planetary materials. With only two stable, light isotopes, it is impossible to determine the source of observed fractionations, and there is great overlap in C isotopic composition among carbonaceous chondrites, ordinary chondrites, and differentiated materials including ureilites (Grady and Wright, 2003).

Rankenburg et al. (2007) interpreted osmium isotopic data to support a linkage between ureilites and carbonaceous chondrites. This Os evidence is noteworthy but far from conclusive. It is true that the ureilites' mean ^{187}Os/^{188}Os is closer to the mean for carbonaceous chondrites than to the means for enstatite and ordinary chondrites. A complication is that ^{187}Os forms as a decay

product of rhenium (^{187}Re). Rankenburg et al. (2007) opined that the "narrow range" of ureilite ^{187}Os/^{188}Os shows that little Re/Os fractionation occurred during the early igneous processing, but the relative Re/Os ratios (noncarbonaceous chondrites higher than the ureilite mean) are such that minor Re/Os depletion cannot be ruled out. Moreover, for constraining the pedigree of ureilites, the ^{187}Os/^{188}Os data (summarized in Fig. 2 of Rankenburg et al.) are not highly systematic. Of 22 ureilite analyses, two have ^{187}Os/^{188}Os lower than any of 13 ordinary chondrites, but two others have ^{187}Os/^{188}Os higher than any of 14 carbonaceous chondrites. In short, the ranges show great overlap, in contrast with the unequivocal evidence from ε^{50}Ti vs. ε^{54}Cr (Fig. 4) and Δ^{17}O vs. ε^{54}Cr (Fig. 5).

4. DISCUSSION

4.1. The host phases for Ti, Cr and Ni within ureilites

In using isotopes of Ti, Cr and Ni to constrain ureilite derivation, ideally we would like to infer the accretionary component(s) that dominantly contributed each of these elements. The original, accretionary carrier phases may have been very different from the final host phases. Still, it is worthwhile to consider the evidence concerning the present hosting phases. The mineralogy of ureilites, based on many separate samples, has been reviewed by, e.g., Mittlefehldt et al. (1998). Additional mineral analyses have been published by Singletary and Grove (2003) and Downes et al. (2008). Apart from their complex, carbon-dominated interstitial areas (the so-called "veins"), and their distinctive late reduction rims, ureilites are essentially pure olivine + pyroxene.

The host phase issue is least clear for titanium, but its main host is probably pyroxene. Ureilite pigeonite has an average TiO_2 content of 0.08 wt%. The extreme low is reportedly 0.02 wt%, in ALH 81101 (Downes et al., 2008). Ureilite high-Ca pyroxenes generally have 0.2–0.3 wt% TiO_2 (Goodrich et al., 2001). Ti-rich phases such as ilmenite, ulvöspinel or armalcolite are unknown from nonpolymict ureilites.

Ureilite chromium is hosted preponderantly in the major minerals olivine and pyroxene. Bulk, non-polymict ureilites consistently have <1.1 wt% "Cr_2O_3" (some of this Cr may actually be divalent). Ureilite olivines typically have 0.6–0.7 wt%. The main ureilite pyroxene, pigeonite, has average Cr_2O_3 content of 1.1 wt%. The extreme low is 0.58 wt%, in EET 87517 (Singletary and Grove, 2003). The high-Ca pyroxenes found in a minority of ureilites have even higher Cr_2O_3. A few ureilites contain traces of Cr-rich sulfide, but in all cases the total Cr in sulfide is much less than the total in mafic silicates.

In contrast, nickel in ureilites is hosted mainly in interstitial (so-called "vein") material. Ureilite bulk-rock Ni averages ~1250 μg/g and ranges from 230 to 2800 μg/g (Warren and Huber, 2006). According to Gabriel (2009; cf. Gabriel and Pack, 2008), ureilite olivines contain only 16–83 μg/g Ni, and ureilite pyroxenes less than 26 μg/g, while the metals of the interstitial areas generally contain 40,000–50,000 μg/g.

Thus, the current host setting for Ni (minor interstitial matter) is very different from the host setting for Cr (the major mafic silicates; probably also true of Ti). The degree to which an analogous difference existed during the accretionary stage of ureilite evolution is not known, but at least at present the full set of observed isotopic peculiarities (versus, e.g., carbonaceous chondrites) cannot be linked to any single minor component.

Ueda et al. (2006) briefly speculated that the ureilites' low ε^{54}Cr may have developed from a CI- or CM-like precursor by selective melting of some ^{54}Cr-rich phase(s) during anatexis. However, during anatexis (and pre-anatectic annealing), as the medium-sized and equant grains of the typical ureilite texture grew, Cr evidently partitioned efficiently into the major minerals olivine and pyroxene, because bulk ureilites are in general not Cr-depleted; they are mildly Cr-enriched, by an average factor of ~2 relative to CI (e.g., Warren and Kallemeyn, 1992; the enrichment factor for Ti is similar, ~1.3). Thus, all but a tiny proportion of the total original Cr remains; and much of that may have equilibrated before its removal, with the fast-diffusing olivine that now, in a typical ureilite, holds about half of the Cr.

4.2. Relationship between initial chondritic carbon content and carbonaceous affinity

It has often been assumed that the ureilites' remarkably high bulk carbon contents link them with the carbonaceous chondrites (Mueller, 1969; Vdovykin, 1970). The average ureilite bulk C content, 3.2 wt%, is exceeded by only one of the major chondrite groups, CI (~4.1 wt%: Wiik, 1969; Jarosewich, 2006; Pearson et al., 2006). The ureilites were at one stage slightly more C-rich than the final ureilites. There is clear mineralogical evidence for slight carbon loss from all ureilites during an episode of "smelting" (FeO reduction accompanied by oxidation of solid carbon into CO_x gas; this episode was associated with the termination of ureilite anatexis; see, e.g., Warren and Rubin, 2010; the amount of C consumed was probably seldom greater than 0.5 wt%; however, some authors argue for additional major smelting during anatexis; e.g., Goodrich et al., 2007).

Despite the name, "carbonaceous" chondrites are far from uniformly C-rich, and their C content is strongly anticorrelated with petrologic type (Fig. 6). For types above 3, petrologic type essentially represents peak temperature of thermal metamorphism, with type 6 representing ~900 °C (e.g., McSween and Labotka, 1993). Arguably the C-poor CV and the even more C-poor CK chondrites are differently metamorphosed samples of the same original material (Greenwood et al., 2010). As igneous restites, the ureilites are, in essence, petrologic type ~8 or 9. Extrapolated to type 8, the clear anticorrelation trend of the carbonaceous chondrites implies a C content of order 0.01 wt%, i.e., too low by a factor of 100.

Although noncarbonaceous chondrites do not include any samples of petrologic type less than 3 (the vast majority are petrologic types 5–6), in Fig. 6 the ordinary chondrites plot along the same anticorrelation trend as the carbonaceous chondrites. That the carbonaceous chondrites, and

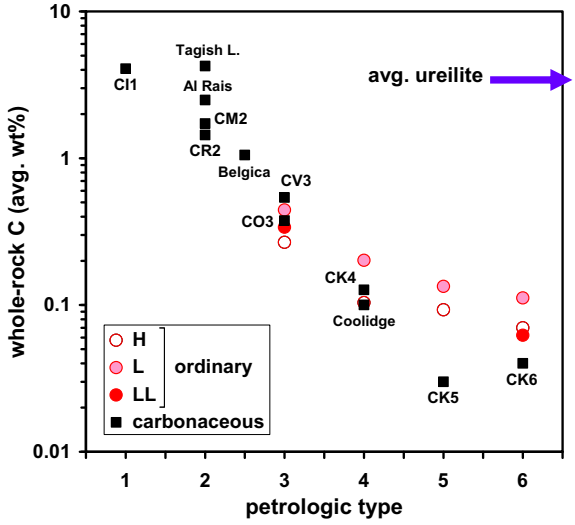

Fig. 6. Carbon concentrations in carbonaceous and ordinary chondrites, plotted versus petrologic type. "Belgica" refers to Belgica 7904. For some of the carbonaceous chondrites (Tagish Lake, Coolidge, CI1 and CK4), in addition to Jarosewich (1990, 2006), data are from Wiik (1969) and Pearson et al. (2006).

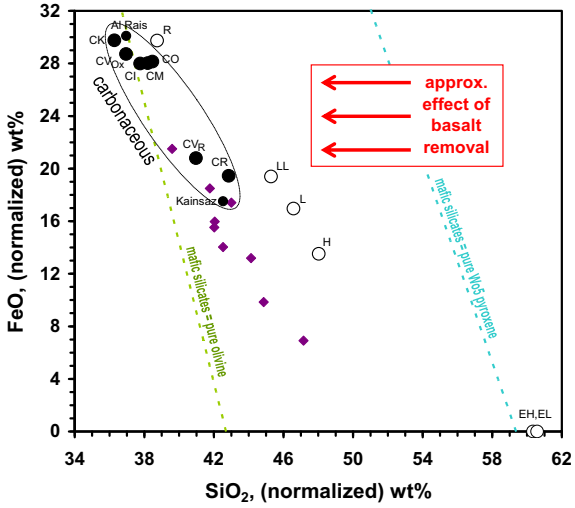

Fig. 7. Variation of SiO_2 and FeO in chondrite and ureilite bulk-nonhydrous-oxide compositions, i.e., the bulk compositions in terms of all oxides, except the extremely volatile H_2O, normalized to 100 wt%. Symbols have same meanings as shown in Fig. 2. As indicated by inset arrows, the effect of basalt removal from peridotite on this diagram is basically to diminish the restite SiO_2 while leaving FeO about the same. As shown by, e.g., Jaques and Green (1980), during low-pressure anatexis (up to pressures far higher than would occur within an asteroid-sized body), among the mafic silicates, pyroxene (high SiO_2) melts, olivine (low SiO_2) does not; and the balance of the melting is dominantly at the expense of feldspar (high SiO_2). In detail, the SiO_2 content of feldspar is proportional to Na content, which feldspathic clasts in polymict ureilites indicate was high (Ikeda et al., 2000; Ikeda and Prinz, 2001; Cohen et al., 2004; Kita et al., 2004; Goodrich et al., 2009). Although the melt has roughly 2× lower (FeO + MgO) than the restite, the melt's FeO/MgO is much higher, so the net effect is to leave the restite's FeO little changed. The "CV_{Ox}" and "CV_R" points represent the oxidized and reduced subgroups of CV (cf. Krot et al., 2004). Kainsaz is shown separately in addition to the CO average, because it is a very uncommonly metal-rich CO. The two available bulk analyses of Kainsaz (Dyakonova, 1964; Ahrens et al., 1973, with FeO calculated based on constraint that sum of these high-precision XRF data should be 100 wt%) are grossly discrepant, but their average (shown) seems roughly in agreement with modal analyses (Fuchs and Olsen, 1973; McSween, 1977). A minor complication is that for SiO_2 in EH chondrites (and also to a lesser extent EL) Jarosewich's (1990) technique probably gave erroneously high values by roughly 1%, because some of the reported "SiO_2" is actually from metal (~24 wt% of the meteorite) with roughly 3 wt% Si.

not the noncarbonaceous, happen to include low metamorphic, C-rich types is a weak argument for linkage with ureilites. No known chondrite, and probably none that survives anywhere in the solar system, combines high carbon content with high petrologic type. In a warming planetesimal, carbon is prone to oxidation and loss as CO_x gas (McSween and Labotka, 1993). Obviously this did not occur in the case of the ureilites, presumably because the original ureilite parent body, in contrast with the carbon-depleted chondrites, achieved a large size, and thus a sufficiently high internal pressure regime to stabilize solid C against oxidation; and, crucially, achieved this large size before it got very hot (Warren, 2008). The abundant water that occurs in the low petrologic type carbonaceous chondrites would be a disadvantage, in this respect, as dissociated water probably tended to oxidize carbon even at low temperature (McSween and Labotka, 1993). The carbon retention requirement does not imply or even strongly suggest that the ureilite precursor matter was carbonaceous in the sense that has long been customary in meteorite classification.

4.3. Implications for and from ureilite petrology

Many models of ureilite petrogenesis start with an assumed carbonaceous-chondritic precursor material (e.g., Rubin, 1988; Ikeda and Prinz, 1993; Kita et al., 2004; Goodrich et al., 2007). In terms of igneous petrology, the salient characteristic of carbonaceous chondrites is that their iron is preponderantly in oxidized form. As a result, the ratio of SiO_2 to the combination of other major oxides is lower than it is in most noncarbonaceous chondrites (Fig. 7; the plotted data have been normalized to have the sum of all oxides, excluding the ultra-volatile H_2O, sum to 100 wt%; i.e., the metal, sulfide and H_2O components are discounted). Carbonaceous chondrites also have systematically higher MgO/SiO_2 compared to noncarbonaceous chondrites (Fig. 8). For the context of silicate anatexis and magmatism, where the major reduced phases, metal and sulfide, probably go their own way as immiscible phases and play little direct role (forming a core?; the possibility of major redox preceding or during anatexis will be discussed below), the anticorrelated variations in FeO and SiO_2 (Fig. 7) are in many ways the most petrologically important. The wide FeO variation among chondrites is basically an effect of nebular redox (e.g., Rubin et al., 1988), and chondritic-oxide *mg* is almost linearly correlated with SiO_2, although the

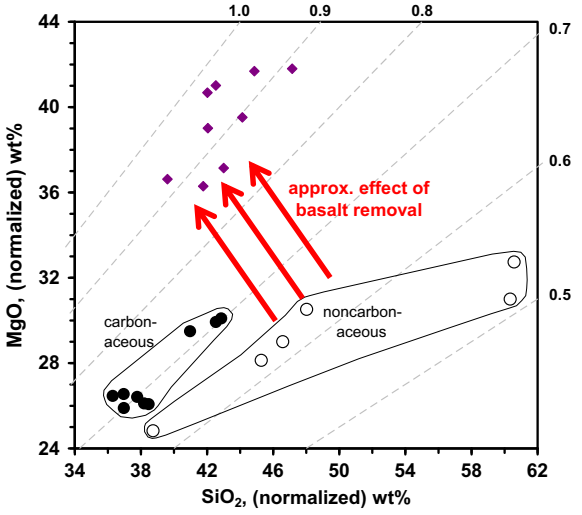

Fig. 8. The ratio MgO/SiO_2 is systematically higher, and the range in SiO_2 content is narrower, among carbonaceous chondrites in comparison to the noncarbonaceous chondrites. Data set and symbols here are same as in Fig. 7. Dashed lines show MgO/SiO_2 (wt ratio) ranging from 0.5 to 1.0.

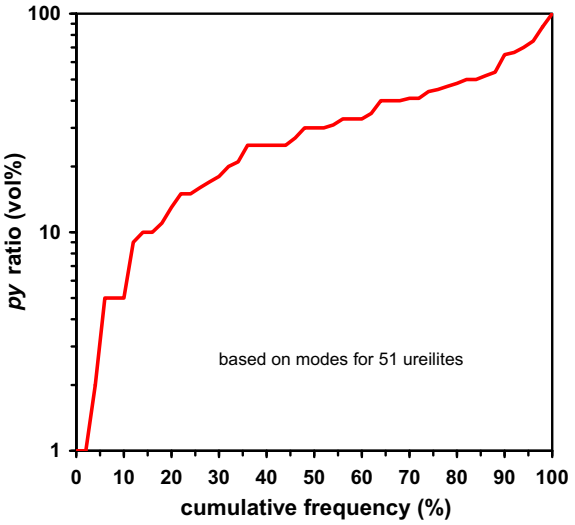

Fig. 9. Distribution of the *py* ratio (≡ pyroxene/[pyroxene + olivine]) among 51 ureilites. Data are mainly from Mittlefehldt et al. (1998).

noncarbonaceous chondrites plot at systematically higher SiO_2, by 3–4 wt%, than the carbonaceous chondrites (Fig. EA-4).

Fig. 7 includes lines to indicate the compositions of pure Mg, Fe olivine and pure Mg, Fe, Ca (Wo5) pyroxene. The position of each chondrite bulk-oxide composition in relation to these lines conveys some idea of the implied bulk olivine/pyroxene ratio, upon equilibration at high temperature and low pressure. Complex chondritic/ureilitic silicates can only be very roughly modeled with this approach, in which the variations of FeO and SiO_2 are linear because the only other free variable is assumed to be MgO, and the sum is fixed at 100 wt%. Assuming a high-Ca composition for the pyroxene, for example, would shift the pyroxene line to lower SiO_2 by several wt%. Moreover, the chondrites are not pure olivine + pyroxene. Clearly, however, compared to the carbonaceous chondrites the noncarbonaceous chondrites show a much wider range of potential bulk-equilibrated *py* (≡ pyroxene/[pyroxene + olivine]), from ~100 wt% for the enstatite chondrites (equilibrated EC are indeed devoid of olivine: Rubin, 1997), to near zero for the R chondrites (Isa et al., 2010). In contrast, for any carbonaceous-chondritic starting material, unless and until a large fraction of the abundant initial Fe-oxide is reduced (or otherwise removed), the SiO_2 content of the oxide-silicate component will remain low, and the mafic silicates will be preponderantly olivine.

As asteroidal mantle restites, the ureilites must have *py* significantly lower than their bulk parent asteroid. Ureilites are extremely depleted, retaining in most cases (ignoring polymict samples) no feldspar whatsoever (or a tiny trace of feldspar in the lone exception, EET 96001: Warren et al., 2006). Yet pyroxene, usually low-Ca (pigeonite), is a major component in the vast majority of ureilites (Fig. 9). Both the average and median *py* for ureilites equals 30 vol%. The simplest explanation for this observation is to assume that the ureilite precursor material was pyroxene-rich, and thus (probably, per Fig. 7) noncarbonaceous.

Consider the composition of the complementary basaltic magma component that was removed from the chondritic ureilite precursor material, as implied by the average ureilite composition U in combination with assumptions for the precursor initial composition I and the proportion f of the (aggregated) partial melting. The mass balance is:

$$I = fL + (1-f)U \quad (1a)$$

$$L = (I - (1-f)U)/f \quad (1b)$$

where I, U and L are in wt% of the oxide, and f is expressed as mass fraction of the initial system. The f in ureilite genesis is generally assumed to have been close to 0.25 (e.g., Warren and Kallemeyn, 1992; Kita et al., 2004; Goodrich et al., 2007), but results from models assuming conservatively higher range in f are shown in Fig. 10 and Table EA-2. Assuming a simple partial melting model is valid, the L composition shown in Fig. 10 for the various chondrite varieties should plot among the basaltic (Al-rich) materials from polymict ureilites that are shown for comparison. There is no assurance that these minor basaltic components are highly representative of the overall lost basalt component, but their average SiO_2 (59 wt%) and FeO (7 wt%) are also broadly consistent with compositions implied for five additional clasts by the mineralogical data of Cohen et al. (2004). The high Na content typical of ureilitic plagioclase (Cohen et al., 2004; Goodrich et al., 2004) implies a relatively high SiO_2 in comparison with the Na-poor plagioclase of some other extraterrestrial basalts (e.g., eucrites, angrites).

For any carbonaceous-chondritic I, Fig. 10 indicates that the "lost" basalt L must have higher FeO and lower SiO_2 than most of the ureilitic basaltic materials. Agreement between the ureilitic basaltic materials and L in Fig. 10 is more satisfactory if I is similar (in these

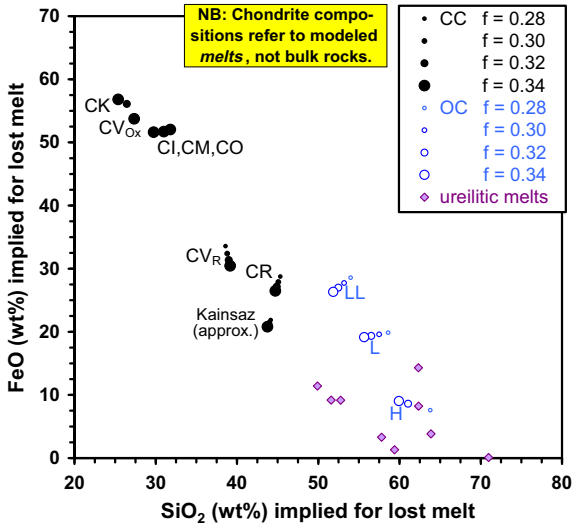

Fig. 10. Results implied by Eq. (1) for SiO_2 and FeO in aggregate of "lost" basaltic melt complementary to the average ureilite, assuming that ureilites represent partial-melting restites. The average ureilite composition used for this modeling (see Table EA-1) is based on data from Wiik (1969), Jarosewich (1990) and Yanai et al. (1995). Shown here are results from a straightforward partial melting model. For most of the carbonaceous chondrite varieties, models are shown only for high *f* because smaller *f* results in impossibly negative melt MgO concentration. See Fig. EA-5 for results from models that assume partial melting was accompanied by major smelting. Data for feldspathic clasts and glasses within polymict-brecciated ureilites (two defocused-beam clast analyses, five "trapped" magmatic glass compositions, and two glass analyses from glass-dominated clasts) are from Ikeda and Prinz (2001), Kita et al. (2004) and Goodrich et al. (2009). Mesostasis-like glasses, interstitial to larger crystalline silicate components (Ikeda et al., 2000; Kita et al., 2004) were excluded from this data set. Composition shown for the CO_3 Kainsaz is "approx" because it represents an average of two grossly discrepant analyses; see caption of Fig. 7.

admittedly limited aspects) to an ordinary chondrite. A similar conclusion that the starting composition (*I*) probably had an OC-like MgO/SiO_2 was reached by Goodrich (1999) based on a more complex forward modeling approach: combining the assumed *I* with various petrologic parameters (much more than simply *f*) to predict both residue (*U*) and melt (*L*) compositions. However, Goodrich (1999) also concluded that the starting (*I*) Ca/Al ratio must have been enriched by a large factor (~3.5× chondritic, for an *I* otherwise based on OC silicates), whereas I draw no such inference. The *L* compositions derived from OC-based *I* models in Table EA-2 (and analogous models assuming slightly lower *f*) have plausible Al_2O_3 and CaO contents without invoking any pre-anatectic fractionation of Ca/Al.

The simple partial melting process would alter *py* and *mg* in systematic ways (always lowering *py*; always raising *mg*) and to only limited extents. To account for the great diversity of ureilites in these parameters (Fig. 9 shows *py*; Fig. 1 shows *mg*), the parent asteroid must have accreted a diverse mélange in terms of initial *py* and *mg* (cf. Goodrich and Delaney, 2000) as well as oxygen-isotopic composition (Clayton and Mayeda, 1988).

An alternative and long-popular model of ureilite petrogenesis assumes that the ureilite anatexis involved major "smelting" (FeO reduction with C oxidation during melting) (e.g., Singletary and Grove, 2003, 2006; Goodrich et al., 2007; Wilson et al., 2008). In principle, even with an assumed carbonaceous-chondrite-like precursor material, provided sufficient smelting occurs during anatexis the mass balance might be satisfactory for the "lost" basaltic component (Fig. EA-5; cf. Goodrich, 1999). A highly localized, disequilibrium, abortive form of impact "smelting" undoubtedly occurred to varying degrees in all ureilites, usually localized in olivine rims; in rare cases concentrated in pyroxenes (Warren and Rubin, 2010). But this "smelting" occurred in conjunction with an impact disruption of the parent asteroid that caused sudden pressure reduction and rapid cooling, which in turn terminated the anatexis (Warren and Huber, 2006; Herrin et al., 2010). The stable-isotopic evidence discussed above militates against a carbonaceous-chondritic precursor material, and among the known noncarbonaceous chondrites, only the R chondrites have the high FeO consistent with the anatectic smelting model. However, the R chondrites are not remotely ureilite-like in terms of oxygen isotopes (Figs. 5 and EA-1). Moreover, as discussed by Warren and Huber (2006) and Warren (2010), there are numerous reasons to doubt that major smelting occurred during the ureilite anatexis. For example, one line of evidence can be quickly described: The abundant Fe-metal that the smelting model inevitably forms is consistently lacking in the ureilites, and yet they retain highly siderophile elements (e.g., Ir, Os) that inevitably partition into Fe-metal, in near-chondritic proportions (Warren and Huber, 2006; Rankenburg et al., 2007). The siderophile depletion constraint can be met by postulating that the precursor material (in reality a mix of diverse materials) was noncarbonaceous, avoided anatectic smelting, and tended to resemble LL chondrites in having relatively low metal abundance (average 3.8 wt%: Jarosewich, 1990); although of course not in all other respects, such as oxygen-isotopic composition.

4.4. Oxygen, once again

As discussed in Section 3.1, the ureilites' strongly negative $\Delta^{17}O$ is arguably evidence in favor of the carbonaceous chondrite derivation hypothesis. Having discussed the major-element compositional implications of a carbonaceous-chondritic derivation, we have gained some further perspective regarding that $\Delta^{17}O$ evidence.

No noncarbonaceous variety of chondrite except the K (Kakangari) grouplet plots below the TFL on Fig. EA-1. However, among differentiated meteorites, ureilites are not the only type that has negative $\Delta^{17}O$. The types that plot below the TFL include the most abundant and well-sampled variety of achondrite, the HEDs, which cluster in $\Delta^{17}O$ at −0.24 (Wiechert et al., 2004; Greenwood et al., 2005; Scott et al., 2009). The HEDs come from a body well documented to contain abundant pyroxene. A few olivine-bearing diogenites are of great interest (e.g., Beck and McSween, 2010), but the howardites, which are basically mixtures of eucrites and diogenites, at an average mixing

ratio of 2:1 (Warren et al., 2009), only contain on average 1.4 wt% olivine (Delaney et al., 1984). Even before the advent of all the other stable-isotopic constraints discussed above, an assessment of the HED asteroid's bulk composition with heavy emphasis on oxygen isotopes suggested a 70:30 mix of ordinary (H) and carbonaceous (CM) chondritic material (Boesenberg and Delaney, 1997). Fig. 5 suggests that the Main Group pallasites, with $\Delta^{17}O$ of −0.37, are also of noncarbonaceous derivation. The newly discovered NWA 6693 achondrite contains 70 vol% pyroxene and has a *py* ratio of 82 vol%, and its $\Delta^{17}O$ is −1.08 (Warren et al., 2011; unfortunately no other stable isotopic system has yet been analyzed). The overall data base indicates that many bodies exist in this solar system that consist mainly of noncarbonaceous material, and yet plot below the TFL on Fig. EA-1.

4.5. Exceptions that prove the rule

The distribution of the planetary materials on Figs. 4 and 5 is strongly bimodal, with two obviously distinct clusters for the various carbonaceous versus noncarbonaceous materials. The significance of this bimodality becomes slightly clearer through consideration of a few meteorites that are in some ways aberrant in their stable-isotopic characteristics. In Fig. 5, the Eagle Station pallasites plot far from all other metal-rich differentiated materials. The metal-rich chondrite GRO95551 superficially resembles CB (Bencubbin group) carbonaceous chondrites, yet it plots far from all carbonaceous materials. In Figs. 4 and 5 and EA-3, the basaltic achondrite NWA 011 plots far from the other basaltic planetary materials (Earth, Moon and Mars basalts, HEDs, angrites, the basaltic components of mesosiderites). In each of these cases, the isotopic result, despite being unusual, holds true to form in the sense that the aberrant compositions avoid the gap between the carbonaceous and noncarbonaceous material types; i.e., instead of reducing the gap, Eagle Station and NWA 011 plot squarely in the carbonaceous region, and GRO 95551 plots squarely in the noncarbonaceous region. The ureilites, by plotting far from the similarly carbon-rich CI chondrites, arguably constitute yet another "exception". As more analyses are acquired in the future, it will be interesting to see how well this isotope-compositional bimodality withstands growth in the compositional-petrological diversity of the analyzed materials. Table EA-1 indicates some obvious shortcomings of the existing data base.

4.6. Evidence of mixing within and between isotopic reservoirs

Carbonaceous chondrites show isotopic evidence for mixing of several fundamentally different components. Their calcium–aluminum-rich inclusions (CAI) feature extremely high $\varepsilon^{50}Ti$ along with extremely low $\Delta^{17}O$ (Trinquier et al., 2009; Clayton, 2008). However, in the CAI-rich CV3 Allende, chondrules have low $\varepsilon^{50}Ti$, overlapping, in two cases, the noncarbonaceous (whole-rock) range (Trinquier et al., 2009). To a large extent, the trends among the carbonaceous chondrites in Figs. 4 and 5 probably reflect mixing between their CAI and other components. However, CAI are far from the whole story. Dauphas et al. (2010) and Qin et al. (2011) found that in the CI1 Orgueil (and probably also the CM2 Murchison) enrichments in ^{54}Cr are linked with presolar oxides, most likely Cr-spinels, of order 10–100 nm in size. CAI are probably too poor in Cr to have a dominant influence on $\varepsilon^{54}Cr$ in bulk chondrites (Qin et al., 2010a). In Figs. 4 and 5, the carbonaceous-chondritic mixing trend is aligned such that neither the CAI-rich end (i.e., CV and CK, with low $\varepsilon^{54}Cr$ and high $\varepsilon^{50}Ti$) nor the CAI-poor end (CI; high $\varepsilon^{54}Cr$ and low $\varepsilon^{50}Ti$) is appreciably closer than the middle of the trend (CB, CM, CR) to the cluster of the noncarbonaceous planetary materials.

The remarkably wide range in $\varepsilon^{62}Ni$ found by Regelous et al. (2008) among four IVB irons, from −0.005 to 0.174 (± 0.056), may be another reflection of mixing, but unfortunately the utility of $\varepsilon^{62}Ni$ for constraining the mixing issue is still limited, partly due to high uncertainty of the analyses. No $\varepsilon^{54}Cr$ or $\varepsilon^{50}Ti$ data are available for IVB irons. For ureilites, Quitté et al. (2010) found slight differences in $\varepsilon^{60}Ni$ and $\varepsilon^{61}Ni$ between bulk and silicate compositions, which these authors interpreted as reflecting an unspecified mixing process. Gabriel and Pack (2008; using the same data in abstract form) argued for late injection of metal with $\varepsilon^{60}Ni \sim 0$ into silicates with $\varepsilon^{60}Ni$ of roughly −0.4. However, by far the most precisely measured data pair (for EET 87517) shows no significant difference between bulk and silicate $\varepsilon^{60}Ni$.

Although these data, especially the $\varepsilon^{50}Ti$ data of Trinquier et al. (2009) for Allende chondrules, indicate that the mixing processes were complex, and separation between the carbonaceous and noncarbonaceous environments was far from total, the overall evidence still suggests that separation between the two reservoirs prevailed to a remarkably efficient extent. Allende's whole-rock $\varepsilon^{50}Ti$ has been determined by eight separate analyses (Leya et al., 2008; Trinquier et al., 2009), and the lowest result, 2.5, is far higher than the nearest noncarbonaceous whole-rock material (Earth, at 0.07). Allende's whole-rock $\varepsilon^{54}Cr$ has also been determined by eight separate analyses (Shukolyukov and Lugmair, 2006b; Trinquier et al., 2009; de Leuw et al., 2010; Qin et al., 2010a), and the results range from 0.85 to 1.30, showing no overlap with even the extreme high $\Delta^{17}O$, high $\varepsilon^{54}Cr$ end ($\varepsilon^{54}Cr = 0.43$, for R chondrites) of the noncarbonaceous range.

4.7. Nonindigenous components in polymict ureilites

As reviewed by Goodrich et al. (2004), polymict ureilites generally (with the glaring exception of the recently fallen Almahata Sitta: Bischoff et al., 2010) contain only minor (~1%) proportions of materials not apparently indigenous to the original ureilite parent body. The nonindigenous materials include clasts of suspected angritic affinity, a variety of chondritic clasts that appear to be dominantly ordinary-chondritic, one of apparent R chondrite affinity, but also a variety of dark clasts that resemble carbonaceous chondrite matrix materials. Goodrich et al. (2004) cautioned against the notion that one of these sparse chondritic-clastic materials may have some special link with

ureilites, and noted that the nonindigenous materials are too low in abundance, and too heterogeneously distributed, for relative abundances to be meaningfully constrained.

In the case of Almahata Sitta, the nonindigenous component is major (Bischoff et al., 2010), and thus may reflect a fundamentally different manner of admixture (e.g., gentler, less disruptive collisions); so the nature of the predominant nonindigenous component might be significant. Bischoff et al. (2010) found that among 40 separate fragments they studied, 23 are ureilitic but 17 are chondritic. Those 17 comprise seven EL chondrites, three impact-melted EL chondrites, one EH chondrite, three impact-melted EH chondrites, two H chondrites, and one sample of a chondrite that is ungrouped but shows affinity with R chondrites. Zolensky et al. (2010) found four (additional?) chondritic pieces, comprising one each of L, H, EL and EH. Thus, 21 (or slightly fewer) separate chondritic clasts are exclusively noncarbonaceous, albeit a wide variety of lithologies are represented. If, as suggested by Bischoff et al. (2010), this mixing occurred early, during the reaccretion of the ureilites into a second-generation parent body after the catastrophic disruption of the original ureilite body (e.g., Warren and Kallemeyn, 1992; Goodrich et al., 2004; Herrin et al., 2010), then the acquisition of diverse yet consistently noncarbonaceous chondritic materials may be another indication that the original body was within a portion of the solar system dominated by noncarbonaceous materials.

4.8. The spatial provenance of ureilites and other planetary materials

Pronounced compositional bimodality (Figs. 4 and 5) is most simply explained by a model of binary, disparate origins. In the context of the early solar system, one obvious and fundamental potential divergence between two modes of origin is spatial, between the inner solar system (sunward relative to Jupiter) and the outer solar system. However, the current derivation location of most chondrites is the asteroid belt, at 2–4 AU, between Mars and Jupiter. Dark, "C" (for carbonaceous) type asteroids predominate in the outer belt (e.g., Bus and Binzel, 2002; for a specific conjectured connection to ureilites: Hartmann et al., 2011). A common assumption (e.g., Bizzarro et al., 2007; Qin et al., 2010a) is that all the chondrites formed in the inner solar system, albeit the carbonaceous chondrites formed relatively farthest from the Sun. Compositional diversity among the primitive planetary materials (chondrites) may have developed primarily as an effect of temporally episodic accretion of the solar nebula (de Leuw et al., 2010).

Many of the carbonaceous chondrites, such as CV and CO, are nearly anhydrous, and the location of the "snow line" in the relevant (mature) phase of a protoplanetary nebula is believed to be well inside of Jupiter (Lacar et al., 2006; Garaud and Lin, 2007; Kennedy and Kenyon, 2008). However, the snow line (or front) may not have been as simple as commonly portrayed in nebular models. In the judgment of Wood (2005; his Fig. 2), all of the carbonaceous chondrites (or anyway, the groups CI, CM, CR, CO and CV) formed beyond the snow line; and even the ordinary chondrites formed partially beyond it.

Weissman et al. (2002) concluded from dynamical considerations that comet orbits frequently evolve into asteroidal orbits, that $\sim 6 \pm 4\%$ "or perhaps more" of the near-Earth asteroidal population is derived from Jupiter-family comets, and that it is "highly likely that many asteroids in eccentric orbits with large semi-major axes and large inclinations are derived from the Oort cloud." Gounelle et al. (2006) found that the only known orbit for a carbonaceous chondrite, the CI Orgueil, was most closely matched by the orbits of Jupiter-family comets. From the perspective of Figs. 4 and 5, it is hard to believe that the CI and CM carbonaceous chondrites could be products of the outer solar system, as suggested by Gounelle et al. (2008; cf. Wasson, 1976), and yet the other (CV–CO–CK–CR–CB) carbonaceous chondrites come from the inner solar system, with the noncarbonaceous chondrites and nearly all of the differentiated materials. Going beyond Gounelle et al. (2008), I speculate that possibly all of the carbonaceous chondrites may have originally accreted in the outer solar system. Although admittedly conjectural, this hypothesis is testable through discovery and analysis of additional types of planetary materials (cf. Table EA-1).

Very recently, Walsh et al. (2011) have suggested that as a consequence of radial migration and mass growth of the giant planets, the belt region (i.e., today's meteorite source region) underwent a complex evolution that culminated in a significant inward migration of planetesimals from the outer solar system into the belt (mainly the outer belt) region. Walsh et al. (2011) estimate that the final belt, after modification (mainly depletion) in consequence of much later catastrophic migration among the giant planets (the Nice model: Gomes et al., 2005), consists of 1/4 "S-type" matter that originated from the inner solar system, and 3/4 "C-type" material derived from the outer solar system. Even without the primordial migration effects assumed by Walsh et al. (2011), major addition of outer solar system material into the belt region appears to be a corollary of the Nice model (Levison et al., 2009).

In any event, despite the mixed message from oxygen isotopes, the stable-isotopic constraints as a whole, and particularly ε^{54}Cr in combination with ε^{50}Ti (Fig. 4) and ε^{54}Cr in combination with Δ^{17}O (Fig. 5), suggest that the ureilites represent fundamentally the same noncarbonaceous mode of material as the inner solar system bodies Earth, the Moon, Mars and the HED asteroid.

5. CONCLUSIONS

1. The most revealing evidence concerning the dominant pedigree of the mix of ureilitic precursor materials is probably the plot of ε^{50}Ti vs. ε^{54}Cr, followed closely by Δ^{17}O vs. ε^{54}Cr. In both cases, the ureilite compositions cluster far from and in a direction approximately orthogonal to a trend internal to the carbonaceous chondrites. Notwithstanding the impressive resemblance to

carbonaceous chondrites in terms of diversely ^{16}O-rich oxygen, the ureilite precursors accreted from preponderantly non-"carbonaceous" materials.

2. For distinguishing between carbonaceous and noncarbonaceous derivation, simple consideration of oxygen isotopic composition in relation to the TFL is insufficient. The CI chondrites have positive Δ^{17}O (as previously known), and the exception they pose with respect to the TFL criterion is tiny compared to the extent (-1.0‰ on average, -2.4‰ at full range) to which the noncarbonaceous ureilites have negative Δ^{17}O.
3. The high carbon contents of the low petrologic type carbonaceous chondrites only weakly link them with ureilites, because ureilites as anatectic restites are equivalent to a very high petrologic type, perhaps 8 or 9; and high petrologic type carbonaceous chondrites are no more C-rich than their noncarbonaceous counterparts. The reason for high accretion of C into the ureilite parent asteroid is not known, but its retention (against oxidation) was presumably caused by attainment of high internal pressures in advance of high internal temperatures.
4. To account for the great diversity of ureilites in modal *py* and silicate-core *mg*, the parent asteroid must have accreted a diverse mélange of noncarbonaceous materials.
5. The noncarbonaceous chondrites have relatively low MgO/SiO_2 and include varieties with moderate FeO, and thus appear better suited than the carbonaceous chondrites to be sources of moderate-*py* mantle restites like the ureilites (average 30 vol%), without requiring major reduction of FeO by smelting.
6. The striking bimodality of planetary materials on the ε^{50}Ti vs. ε^{54}Cr and Δ^{17}O vs. ε^{54}Cr diagrams may represent an extreme manifestation of heterogeneous accretion within the protoplanetary disk, but I speculate that it might correspond to a division between materials that originally accreted in the outer solar system (carbonaceous) and materials that accreted in the inner solar system (everything noncarbonaceous, including the ureilites).

ACKNOWLEDGMENTS

The author thank A. Trinquier, C.A. Goodrich and Anonymous for insightful reviews; also J. Isa, C. Koeberl, A.E. Rubin, and especially J.T. Wasson for helpful advice. This work was supported by NASA Grants NNX09AE31G and NNX09AM65G.

APPENDIX A. SUPPLEMENTARY DATA

Supplementary data associated with this article can be found, in the online version, at doi:10.1016/j.gca.2011.09.011.

REFERENCES

Ahrens L. H., Willis J. P. and Erlank A. J. (1973) The chemical composition of Kainsaz and Efremovka. *Meteoritics* **8**, 133–139.

Beck A. W. and McSween, Jr., H. Y. (2010) Diogenites as polymict breccias composed of orthopyroxenite and harzburgite. *Meteorit. Planet. Sci.* **45**, 850–872.

Berkley J. L., Taylor G. J., Keil K., Harlow G. E. and Prinz M. (1980) The nature and origin of ureilites. *Geochim. Cosmochim. Acta* **44**, 1579–1597.

Bischoff A., Horstmann M., Pack A., Laubenstein M. and Haberer S. (2010) Asteroid 2008 TC3 – Almahata Sitta: a spectacular breccia containing many different ureilitic and chondritic lithologies. *Meteorit. Planet. Sci.* **45**, 1638–1656.

Bizzarro M., Ulfbeck D., Trinquier A., Thrane K., Connelly J. N. and Meyer B. S. (2007) Evidence for a late supernova injection of ^{60}Fe into the protoplanetary disk. *Science* **316**, 1178–1181.

Boesenberg J. S. and Delaney J. S. (1997) A model composition of the basaltic achondrite planetoid. *Geochim. Cosmochim. Acta* **61**, 3205–3225.

Bogdanovski O. and Lugmair G. W. (2004) Manganese–chromium isotope systematics of basaltic achondrite Northwest Africa 011. *Lunar Planet. Sci.* **35**, #1715 (abstr.).

Boynton W. V., Starzyk P. M. and Schmitt R. A. (1976) Chemical evidence for the genesis of the ureilites, the achondrite Chassigny and the nakhlites. *Geochim. Cosmochim. Acta* **40**, 1439–1447.

Bus S. J. and Binzel R. P. (2002) Phase II of the small main belt asteroid spectroscopic survey: a feature-based taxonomy. *Icarus* **158**, 146–177.

Choi B.-G., Ahn I., Ziegler K., Wasson J. T., Young E. D. and Rubin A. E. (2009) Oxygen isotopic compositions and degree of alteration of CR chondrites. *Meteorit. Planet. Sci.* **44**, A50 (abstr.).

Clayton R. N. (2008) Oxygen isotopes in the early solar system – a historical perspective. *Rev. Mineral. Geochem.* **68**, 5–14.

Clayton R. N. and Mayeda T. K. (1988) Formation of ureilites by nebular processes. *Geochim. Cosmochim. Acta* **52**, 1313–1318.

Clayton R. N. and Mayeda T. K. (1996) Oxygen isotope studies of achondrites. *Geochim. Cosmochim. Acta* **60**, 1999–2017.

Clayton R. N., Grossman L. and Mayeda T. K. (1973) A component of primitive nuclear composition in carbonaceous meteorites. *Science* **182**, 485–488.

Clayton R. N., Onuma N. and Mayeda T. K. (1976) A classification of meteorites based on oxygen isotopes. *Earth Planet. Sci. Lett.* **30**, 10–18.

Clayton R. N., Mayeda T. K., Goswami J. N. and Olsen E. J. (1991) Oxygen isotope studies of ordinary chondrites. *Geochim. Cosmochim. Acta* **55**, 2317–2337.

Cohen B. A., Goodrich C. A. and Keil K. (2004) Feldspathic clast populations in polymict ureilites: stalking the missing basalts from the ureilite parent body. *Geochim. Cosmochim. Acta* **68**, 4249–4266.

Dauphas N., Cook D. L., Sacarabany A., Froehlich C., Davis A. M., Wadwha M., Pourmand A., Rauscher T. and Gallino R. (2008) Iron 60 evidence for early injection and efficient mixing of stellar debris in the protosolar nebula. *Astrophys. J.* **686**, 560–569.

Dauphas N., Remusat L., Chen J. H., Roskoz M. M., Papanastassiou D. A., Stodolna J., Guan Y. and Ma C. (2010) Neutron-rich chromium isotope anomalies in supernova nanoparticles. *Astrophys. J.* **720**, 1577.

de Leuw S., Papanastassiou D. and Wasson J. T. (2010) Chromium isotopes in chondrites and the heterogeneous accretion of the solar nebula. *Lunar Planet. Sci.* **41**, #2703 (abstr.).

Delaney J. S., Prinz M. and Takeda H. (1984) The polymict eucrites. *Proc. Lunar Planet. Sci. Conf.* **15**, C251–C288.

Downes H., Mittlefehldt D. W., Kita N. and Valley J. W. (2008) Evidence from polymict ureilite meteorites for a disrupted and re-accreted single ureilite parent asteroid gardened by several distinct impactors. *Geochim. Cosmochim. Acta* **72**, 4825–4844.

Dyakonova M. I. (1964) Chemical analyses of meteorites from the collection of the Committee for Meteorites, Acad. Sci. USSR. *Meteoritika* **25**, 129–132.

Franchi I. A., Sexton A. S., Wright I. P. and Pillinger C. T. (1998) Oxygen isotopic homogeneity in the ureilite population. *Lunar Planet. Sci.* **29**, #1685 (abstr.).

Fuchs L. H. and Olsen E. (1973) Composition of metal in type III carbonaceous chondrites and its relevance to the source-assignment of lunar metal. *Earth Planet. Sci. Lett.* **18**, 379–384.

Gabriel A. D. (2009) *Origin and Evolution of Ureilite Vein Metal – Fe, Ni, Co and Ni Isotope Systematics of Ureilite Vein Metal and Ureilite Silicates*. Doctoral Thesis, Univ. Göttingen, 215pp.

Gabriel A. D. and Pack A. (2008) Fe, Co and Ni in ureilite metal and silicates. *Lunar Planet. Sci.* 39, #1391 (abstr.).

Garaud P. and Lin D. N. C. (2007) The effects of internal dissipation and surface irradiation on the structure of disks and the location of the snow line around Sun-like stars. *Astrophys. J.* **654**, 606–624.

Gomes R., Levison H. F., Tsiganis K. and Morbidelli A. (2005) Origin of the cataclysmic Late Heavy Bombardment period of the terrestrial planets. *Nature* **435**, 466–469.

Goodrich C. A. (1992) Ureilites: a critical review. *Meteoritics* **27**, 327–352.

Goodrich C. A. (1999) Are ureilites residues from partial melting of chondritic material? The answer from MAGPOX. *Meteor. Planet. Sci.* **34**, 109–119.

Goodrich C. A. and Delaney J. S. (2000) Fe/Mg–Fe/Mn relations of meteorites and primary heterogeneity of primitive achondrite parent bodies. *Geochim. Cosmochim. Acta* **64**, 2255–2273.

Goodrich C. A., Jones J. H. and Berkley J. L. (1987) Origin and evolution of the ureilite parent magmas: multi-stage igneous activity on a large parent body. *Geochim. Cosmochim. Acta* **51**, 2255–2273.

Goodrich C. A., Fioretti A. M., Tribaudino M. and Molin G. (2001) Primary trapped melt inclusions in olivine in the olivine-augite-orthopyroxene ureilite Hughes 009. *Geochim. Cosmochim. Acta* **65**, 621–652.

Goodrich C. A., Krot A. N., Scott E. R. D., Taylor G. J., Fioretti A. M. and Keil K. (2002) Formation and evolution of the ureilite parent body and its offspring. *Lunar Planet. Sci.* **33**, #1379 (abstr.).

Goodrich C. A., Scott E. R. D. and Fioretti A. M. (2004) Ureilitic breccias: clues to the petrologic structure and impact disruption of the ureilite parent asteroid. *Chem. Erde* **64**, 283–327.

Goodrich C. A., Van Orman J. A. and Wilson L. (2007) Fractional melting and smelting on the ureilite parent body. *Geochim. Cosmochim. Acta* **71**, 2876–2895.

Goodrich C. A., Fioretti A. M. and van Orman J. (2009) Petrogenesis of the augite-bearing ureilites Hughes 009 and FRO 90054/93008 inferred from melt inclusions in olivine, augite and orthopyroxene. *Geochim. Cosmochim. Acta* **73**, 3055–3076.

Gounelle M., Spurný P. and Bland P. A. (2006) The atmospheric trajectory and orbit of the Orgueil meteorite. *Meteor. Planet. Sci.* **41**, 135–150.

Gounelle M., Morbidelli A., Bland P. A., Spurny P., Young E. D. and Sephton M. (2008) Meteorites from the outer solar system? In *The Solar System Beyond Neptune* (eds. H. Boehnhardt, D. P. Cruikshank, A. Morbidelli and M. A. Barucci). The University of Arizona Press, pp. 525–541.

Grady M. M. and Wright I. P. (2003) Elemental and isotopic abundances of carbon and nitrogen in meteorites. *Space Sci. Rev.* **106**, 231–248.

Greenwood R. C., Franchi I. A., Jambon A. and Buchanan P. C. (2005) Widespread magma oceans on asteroidal bodies in the early solar system. *Nature* **435**, 916–918.

Greenwood R. C., Franchi I. A., Kearsley A. T. and Alard O. (2010) The relationship between CK and CV chondrites. *Geochim. Cosmochim. Acta* **74**, 1684–1705.

Hartmann W. K., Goodrich C. A., O'Brien D. P., Michel P., Weidenschilling S. J. and Sykes M. V. (2011) Breakup and reassembly of the ureilite parent body, formation of 2008 TC3/Almahata Sitta, and delivery of ureilites to Earth. *Lunar Planet. Sci.* **42**, #1360 (abstr.).

Herrin J. S., Zolensky M. E., Ito M., Le L., Mittlefehldt D. W., Jenniskens P., Ross A. J. and Shaddad M. H. (2010) Thermal and fragmentation history of ureilitic asteroids: insights from the Almahata Sitta fall. *Meteorit. Planet. Sci.* **45**, 1789–1803.

Higuchi H., Morgan J. W., Ganapathy R. and Anders E. (1976) Chemical fractionations in meteorites – X. Ureilites. *Geochim. Cosmochim. Acta* **40**, 1563–1571.

Ikeda Y. and Prinz M. (1993) Origin of ureilites based on Allende dark inclusions. *NIPR Symp. Antarct. Meteorit.* **XVIII**, 44–46 (abstr.).

Ikeda Y. and Prinz M. (2001) Magmatic inclusions and felsic clasts in the Dar al Gani 319 polymict ureilite. *Meteor. Planet. Sci.* **36**, 481–499.

Ikeda Y., Prinz M. and Nehru C. E. (2000) Lithic and mineral clasts in the Dar al Gani (DAG) 319 polymict ureilite. *Antarctic Meteorite Research* **13**, 177–221.

Isa J., Rubin A. E. and Wasson J. T. (2010) Petrology and bulk chemistry of R chondrites: new data. *Lunar Planet. Sci.* **41**, abstract #2525.

Jaques A. L. and Green D. H. (1980) Anhydrous melting of peridotite at 0–15 Kb pressure and the genesis of tholeiitic basalts. *Contrib. Mineral. Petrol.* **73**, 287–310.

Jarosewich E. (1990) Chemical analyses of meteorites: a compilation of stony and iron meteorite analyses. *Meteoritics* **25**, 323–337.

Jarosewich E. (2006) Chemical analyses of meteorites at the Smithsonian Institution: an update. *Meteorit. Planet. Sci.* **41**, 1271–1419.

Kennedy G. M. and Kenyon S. J. (2008) Planet formation around stars of various masses: the snow line and the frequency of giant planets. *Astrophys. J.* **673**, 502–512.

Kita N. T., Ikeda Y., Togashi S., Liu Y., Morishita Y. and Weisberg M. K. (2004) Origin of ureilites inferred from a SIMS oxygen isotopic and trace element study of clasts in the Dar al Gani 319 polymict ureilite. *Geochim. Cosmochim. Acta* **68**, 4213–4235.

Krot A. N., Keil K., Goodrich C. A., Scott E. R. D. and Weisberg M. K. (2004) Classification of meteorites. In *Treatise on Geochemistry, vol. 1, Meteorites, Comets, and Planets* (ed. A. M. Davis). Elsevier, pp. 83–128.

Lacar M., Podolak M., Sasselov D. and Chiag E. (2006) On the location of the snow line in a protoplanetary disk. *Astrophys. J.* **640**, 1115–1118.

Levison H. F., Bottke W. F., Gounelle M., Morbidelli A., Nesvorny D. and Tsiganis K. (2009) Contamination of the asteroid belt by primordial trans-Neptunian objects. *Nature* **460**, 364–366.

Leya I., Schoenbachler M., Wiechert U., Krahenbuhl U. and Halliday A. N. (2008) Titanium isotopes and the radial heterogeneity of the solar system. *Earth Planet. Sci. Lett.* **266**, 233–244.

Lyons J. R. and Young E. D. (2005) CO self-shielding as the origin of oxygen isotope anomalies in the early solar nebula. *Nature* **435**, 317–320.

Mason B. (1997) GRO 95551 thin section description. *Antarct. Meteorit. Newslett.* **20**(2), 16.

McSween, Jr., H. Y. (1977) Carbonaceous chondrites of the Ornans type – a metamorphic sequence. *Geochim. Cosmochim. Acta* **41**, 477–491.

McSween, Jr., H. Y. and Labotka T. C. (1993) Oxidation during metamorphism of the ordinary chondrites. *Geochim. Cosmochim. Acta* **57**, 1105–1114.

Mittlefehldt D. W., McCoy T. J., Goodrich C. A. and Kracher A. (1998) Non-chondritic meteorites from asteroidal bodies. In *Planetary Materials, Reviews in Mineralogy*, vol. 36 (ed. J. J. Papike). Mineralogical Society of America, pp. 4.1–4.195.

Miyamoto M., Takeda H. and Toyoda H. (1985) Cooling history of some Antarctic ureilites. *Proc. Lunar Planet. Sci. Conf.* **16**, D116–D122.

Mueller G. (1969) Genetical interrelations between ureilites and carbonaceous chondrites. In *Meteorite Research* (ed. P. M. Millman). Reidel, Dordrecht, Holland, pp. 505–517.

Pearson V. K., Sephton M. A., Franchi I. A., Gibson J. M. and Gilmour I. (2006) Carbon and nitrogen in carbonaceous chondrites: elemental abundances and stable isotopic compositions. *Meteorit. Planet. Sci.* **41**, 1899–1918.

Qin L., Alexander C. M., Carlson R. W., Horan M. F. and Yokoyama T. (2010a) Contributors to chromium isotope variation of meteorites. *Geochim. Cosmochim. Acta* **74**, 1122–1145.

Qin L., Rumble D., Alexander C. M., Carlson R. W., Jenniskens P. and Shaddad M. H. (2010b) The chromium isotopic composition of Almahata Sitta. *Meteorit. Planet. Sci.* **45**, 1771–1777.

Qin L., Nittler L. R., Alexander C. M., Wang J., Stadermann F. J. and Carlson R. W. (2011) Extreme ^{54}Cr-rich nano-oxides in the CI chondrite Orgueil – implication for a late supernova injection into the solar system. *Geochim. Cosmochim. Acta* **75**, 629–644.

Quitté G., Markowski A., Latkoczy C., Gabriel A. and Pack A. (2010) Iron-60 heterogeneity and incomplete isotope mixing in the early solar system. *Astrophys. Jour.* **720**, 1215–1224.

Rankenburg K., Brandon A. D. and Humayun M. (2007) Osmium isotope systematics of ureilites. *Geochim. Cosmochim. Acta* **71**, 2402–2413.

Regelous M., Elliott T. and Coath C. D. (2008) Nickel isotope heterogeneity in the early solar system. *Earth Planet. Sci. Lett.* **272**, 330–338.

Ringwood A. E. (1960) The Novo Urei meteorite. *Geochim. Cosmochim. Acta* **20**, 1–4.

Rubin A. E. (1988) Formation of ureilites by impact-melting of carbonaceous material. *Meteoritics* **23**, 333–337.

Rubin A. E. (1997) Mineralogy of meteorite groups. *Meteorit. Planet. Sci.* **32**, 231–247.

Rubin A. E., Fegley B. and Brett R. (1988) Oxidation state in chondrites. In *Meteorites and the Early Solar System* (eds. J. F. Kerridge and M. S. Matthews). The University of Arizona Press, pp. 488–511.

Scott E. R. D., Taylor J. G. and Keil K. (1993) Origin of ureilite meteorites and implications for planetary accretion. *Geophys. Res. Lett.* **20**, 415–418.

Scott E. R. D., Greenwood R. C., Franchi I. A. and Sanders I. S. (2009) Oxygen isotopic constraints on the origin and parent bodies of eucrites, diogenites, and howardites. *Geochim. Cosmochim. Acta* **73**, 5835–5853.

Shukolyukov A. and Lugmair G. W. (2006a) The Mn–Cr isotope systematics in the ureilites Kenna and LEW85440. *Lunar Planet. Sci.* **37**, #1478 (abstr.).

Shukolyukov A. and Lugmair G. W. (2006b) Manganese–chromium isotope systematics of carbonaceous chondrites. *Earth Planet. Sci. Lett.* **250**, 200–213.

Shukolyukov A., Lugmair G. W. and Irving A. J. (2011) Mn–Cr isotope systematics and excess of 54-Cr in metachondrite Northwest Africa 3133. *Lunar Planet. Sci.* **42**, #1527 (abstr.).

Singletary S. J. and Grove T. L. (2003) Early petrogenetic processes on the ureilite parent body. *Meteorit. Planet. Sci.* **38**, 95–108.

Singletary S. and Grove T. L. (2006) Experimental constraints on ureilite petrogenesis. *Geochim. Cosmochim. Acta* **70**, 1291–1308.

Smith C. L., Franchi I. A., Wright I. P., Verchovsky A. B., Grady M. M. and Pillinger C. T. (2001) An integrated mineralogical, petrographic, light stable isotope and noble gas investigation of Sahara 99201 ureilite. *Lunar Planet. Sci.* **32**, #1647 (abstr.).

Takeda H. (1987) Mineralogy of Antarctic ureilites and a working hypothesis for their origin and evolution. *Earth Planet. Sci. Lett.* **81**, 358–370.

Takeda H., Mori H. and Ogata H. (1989) Mineralogy of augite-bearing ureilites and the origin of their chemical trends. *Meteoritics* **24**, 73–81.

Till R. (1974) *Statistical Methods for the Earth Scientist*. Wiley, New York, 154pp.

Trinquier A., Birck J.-L. and Allégre C. J. (2007) Widespread ^{54}Cr heterogeneity in the inner solar system. *Astrophys. J.* **655**, 1179–1185.

Trinquier A., Birck J.-L., Allegre C. J., Gopel C. and Ulfbeck D. (2008) ^{53}Mn–^{53}Cr systematics of the early solar system revisited. *Geochim. Cosmochim. Acta* **72**, 5146–5163.

Trinquier A., Elliott T., Ulfbeck D., Coath C., Krot A. N. and Bizzarro M. (2009) Origin of nucleosynthetic isotope heterogeneity in the solar protoplanetary disk. *Science* **324**, 374–376.

Ueda T., Yamashita K. and Kita N. (2006) Chromium isotopic systematics of ureilite. *NIPR Sympos. Antarct. Meteorit.* **XXX**, 117–118 (abstr.).

Vdovykin G. P. (1970) Ureilites. *Space Sci. Rev.* **10**, 483–510.

Walsh K. J., Morbidelli A., Raymond S. N., O'Brien D. P. and Mandell A. M. (2011) A low mass for Mars from Jupiter's early gas-driven migration. *Nature* **475**, 206–209.

Warren P. H. (2008) A depleted, not ideally chondritic bulk Earth: the explosive-volcanic basalt loss hypothesis. *Geochim. Cosmochim. Acta* **72**, 2217–2235.

Warren P. H. (2010) Asteroidal depth–pressure relationships and the style of the ureilite anatexis. *Meteorit. Planet. Sci.* **45**, A210 (abstr.).

Warren P. H. and Huber H. (2006) Ureilite petrogenesis: a limited role for smelting during anatexis and catastrophic disruption. *Meteorit. Planet. Sci.* **41**, 835–849.

Warren P. H. and Kallemeyn G. W. (1992) Explosive volcanism and the graphite–oxygen fugacity buffer on the parent asteroid(s) of the ureilite meteorites. *Icarus* **100**, 110–126.

Warren P. H. and Rubin A. E. (2010) Pyroxene-selective impact smelting in ureilites. *Geochim. Cosmochim. Acta* **74**, 5109–5133.

Warren P. H., Huber H. and Ulff-Møller F. (2006) Alkali-feldspathic material entrained in Fe, S-rich veins in a monomict ureilite. *Meteorit. Planet. Sci.* **41**, 797–813.

Warren P. H., Kallemeyn G. W., Huber H., Ulff-Møller F. and Choe W. (2009) Siderophile and other geochemical constraints on mixing relationships among HED-meteoritic breccias. *Geochim. Cosmochim. Acta* **73**, 5918–5943.

Warren P. H., Rubin A. E., Isa J., Choi B.-G. and Ahn I. (2011) Northwest Africa 6693, a new type of achondrite: ferroan, sodic, near-ultramafic, and ^{16}O-rich. *Meteor. Planet. Sci.* **46**, A246.

Wasson J. T. (1976) Relative abundance of CM chondrites in the inner and outer solar system. *Meteoritics* **11**, 385 (abstr.).

Wasson J. T. (2000) Oxygen-isotopic evolution of the solar nebula. *Rev. Geophys.* **38**, 491–512.

Wasson J. T., Chou C.-L., Bild R. W. and Baedecker P. A. (1976) Classification of and elemental fractionation among ureilites. *Geochim. Cosmochim. Acta* **40**, 1449–1450.

Weisberg M. K., Prinz M., Clayton R. N., Mayeda T. K., Grady M. M., Franchi I., Pillinger C. T. and Kallemeyn G. W. (1996) The K (Kakangari) chondrite grouplet. *Geochim. Cosmochim. Acta* **60**, 4253–4263.

Weisberg M. K., Prinz M., Clayton R. N., Mayeda T. K., Sugiura N., Zashu S. and Ebihara M. (2001) A new metal-rich chondrite grouplet. *Meteorit. Planet. Sci.* **36**, 401–418.

Weisberg M. K., McCoy T. J. and Krot A. N. (2006) Systematics and evaluation of meteorite classification. In *Meteorites and the Early Solar System II* (eds. D. S. Lauretta and Jr. H. Y. McSween). The University of Arizona Press, Tucson, pp. 19–52.

Weissman P. R., Bottke, Jr., W. F. and Levison H. (2002) Evolution of comets into asteroids. In *Asteroids III* (eds. W. F. Bottke, A. Cellino, P. Paolicchi and R. P. Binzel). The University of Arizona Press, pp. 669–686.

Wiechert U. H., Halliday A. N., Palme H. and Rumble D. (2004) Oxygen isotope evidence for rapid mixing of the HED meteorite parent body. *Earth Planet. Sci. Lett.* **221**, 373–382.

Wiik H. B. (1969) On the regular discontinuities in the composition of meteorites. *Commentationes Phys. Math.* **34**, 135–145.

Wilson L., Goodrich C. A. and Van Orman J. A. (2008) Thermal evolution and physics of melt extraction on the ureilite parent body. *Geochim. Cosmochim. Acta* **72**, 6154–6176.

Wlotzka F. (1972) Haverö ureilite: evidence of recrystallization and partial reduction. *Meteoritics* **7**, 591–600.

Wood J. A. (2005) The chondrite types and their origins. In *Chondrites and the Protoplanetary Disk* (eds. A. N. Krot, E. R. D. Scott and B. Reipurth). Astronomical Society of the Pacific, San Francisco, pp. 953–971.

Yamaguchi A., Clayton R. N., Mayeda T. K., Ebihara M., Oura Y., Miura Y. N., Haramura H., Misawa K., Kojima H. and Nagao K. (2002) A new source of basaltic meteorites inferred from Northwest Africa 011. *Science* **296**, 334–336.

Yamakawa A., Yamashita K., Makashima A. and Nakamura E. (2010) Chromium isotope systematics of achondrites: chronology and isotopic heterogeneity of the inner solar system. *Astrophys. J.* **720**, 150–154.

Yamashita K., Ueda T., Nakamura N., Kita N. and Heaman L. M. (2005) Chromium isotopic study of mesosiderite and ureilite: evidence for ε^{54}Cr deficit in differentiated meteorites. *NIPR Sympos. Antarct. Meteorit.* **1**, 100–101 (abstr.).

Yanai K., Kojima H. and Haramura H. (1995) *Catalog of the Antarctic Meteorites*. National Institute of Polar Research, 230pp.

Yin Q.-Z., Yamashita K., Yamakawa A., Tanaka R., Jacobsen B., Ebel D., Hutcheon I. D. and Nakamura E. (2009) ^{53}Mn–^{53}Cr systematics of Allende chondrules and ε^{54}Cr–δ^{17}O correlation in bulk carbonaceous chondrites. *Lunar Planet. Sci.* **40**, #2006 (abstr.).

Yurimoto H. and Kuramoto K. (2004) Molecular cloud origin for the oxygen isotope heterogeneity in the solar system. *Science* **305**, 1763–1766.

Zolensky M. E., Herrin J., Mikouchi T., Ohsumi K., Friedrich J., Steele A., Rumble D., Fries M., Sandford S., Milam S., Higaya K., Takeda H., Satake W., Kurihara T., Colbert M., Hanna R., Maisano J., Ketcham R., Goodrich C., Le L., Robinson G. A., Martinez J., Ross K., Jenniskens P. and Shaddad M. H. (2010) Mineralogy and petrography of the Almahata Sitta ureilite. *Meteorit. Planet. Sci.* **45**, 1618–1637.

Associate editor: Christian Koeberl